Conformational Study of Tyramine and Its Water Clusters by Laser Spectroscopy

Ilsun Yoon,[†] Kwanyong Seo,[†] Sungyul Lee,[§] Yonghoon Lee,*[,‡] and Bongsoo Kim*[,†]

Department of Chemistry, KAIST, Daejeon 305-701, Korea, College of Environmental Science and Applied Chemistry (BK21), Kyunghee University, Kyungki-do 449-701, Korea, and Advanced Photonics Research Institute, Gwangju Institute of Science and Technology, Gwangju 500-712, Korea

Received: September 26, 2006; In Final Form: January 3, 2007

Tyramine and its monohydrated clusters have been investigated by several laser spectroscopic methods in a pulsed molecular beam. The conformational structures and their effects on hydration have been revealed by resonant two-photon ionization (R2PI), UV−UV ion-dip, and ab initio calculations. UV rotational band contour spectra of the $S_1 \leftarrow S_0$ origin bands enabled determination of ethylamine side chain conformations for all seven stable conformers of tyramine. When coexpanding tyramine with a mixture of Ar and water vapor, we have found two kinds of conformational effects on hydration. One is sensitive to conformation of the ethylamine chain and the other to the orientation of the OH group, particularly in the most stable pair of conformers. UV−UV ion-dip spectra detected seven stable conformers of the monohydrated clusters, of which hydrogen-bonding structures, spectral shifts, and origin band intensity distributions are well explained by considering tyramine as a hybrid of phenylethylamine (PEA) and phenol. Monohydration of the most stable gauche conformer pair (cis and trans) of tyramine leads to more detailed conformational assignments regarding the orientation of the phenolic OH group. Cyclic hydrogen-bonding linkage formed in the monohydrated cluster pair is found to be sensitive to the orientation of the phenolic OH group. One of the cluster pair, in which tyramine has the gauche−cis conformation, is more stabilized by the cyclic hydrogen bonding and its origin band intensity becomes stronger than that of the other.

1. Introduction

Tyramine, *p*-hydroxyphenylethylamine, is formed from the breakdown of protein. Foods high in tyramine are believed to be among the worst migraine triggers. Simple biogenic amines, tyramine and its related molecules (phenylethylamine (PEA), *p*-aminophenylethylamine (*p*-APEA), and *p*-methoxyphenylethylamine (*p*-MPEA)), have the function of neural control.[1] Receptors may recognize molecular conformations of these amines. Understanding their conformations, therefore, can provide valuable insight into their functions in neurotransmission. Laser spectroscopy of isolated molecules and their hydrated clusters in a molecular beam combined with ab initio calculations has proved powerful for studying molecular conformation.[2] Using the R2PI or LIF (laser induced fluorescence) excitation spectra, UV−UV depletion spectroscopy can count the number of stable conformers in the gas phase. The band structures of ground-state vibrational spectrum observed by IR−UV depletion or dispersed fluorescence and fully or partially resolved UV rotational spectrum are strongly dependent on the conformation of flexible biomolecules and their hydrated clusters. Interpretation of various experimental observations and ab initio calculations allows us to understand the conformational hypersurface of biomolecules and their hydrated clusters in detail. Recently, Zwier also showed that we could transfer and measure populations of flexible molecules on the conformational hypersurface.[3]

Teh and Sulkes reported the first LIF excitation spectrum of jet-cooled tyramine and its clusters with several solvent molecules.[4] Martinez et al. observed six distinct conformer origin bands in their LIF excitation spectrum.[5] Because the structure of tyramine is similar to PEA, *p*-APEA, and *p*-MPEA, we may assume that the conformation of tyramine would be similar to those molecules.[6−13] While seven stable conformational structures were observed experimentally in the closely related molecule, *p*-MPEA,[12] only six origin bands have been identified experimentally for tyramine.[5] Most recently, a free-jet microwave study of tyramine was reported by Melandri and Maris.[14] They observed four stable gauche conformers and assigned them on the basis of the relative value of the permanent dipole moment components, μ_b and μ_c, which are sensitive to the relative orientation of the NH_2 and OH groups.

In this work, we have investigated tyramine and its monohydrated clusters in a pulsed molecular beam by R2PI, UV−UV ion-dip, and ab initio calculations. For all seven stable conformers predicted in tyramine, their ethylamine side chain conformations have been determined by the UV rotational band contour spectra. By comparing the origin band intensities corresponding to various tyramine conformers in our R2PI spectra, which were obtained by coexpanding tyramine with pure Ar or a mixture of Ar and water vapor, we have discovered two kinds of conformational effects on hydration. One is sensitive to the conformation of the ethylamine chain and the other to the orientation of the OH group particularly in the most stable pair of conformers. For the monohydrated clusters, seven stable conformers have been counted by UV−UV ion-dip spectra. Their intermolecular hydrogen-bonding structures, spectral shifts, and origin band intensity distributions are well explained by considering tyramine as a hybrid of PEA and phenol. The orientation of the phenolic OH group could not be determined by UV rotational band contour spectra obtained

* To whom correspondence should be addressed. B.K.: Fax: +82-42-869-2810; e-mail: bongsoo@kaist.ac.kr. Y.L.: Fax: +82-62-970-3419; e-mail: lyh@gist.ac.kr.

[†] KAIST.

[‡] Advanced Photonics Research Institute.

[§] Kyunghee University.

10.1021/jp066333l CCC: $37.00
Published on Web 02/22/2007

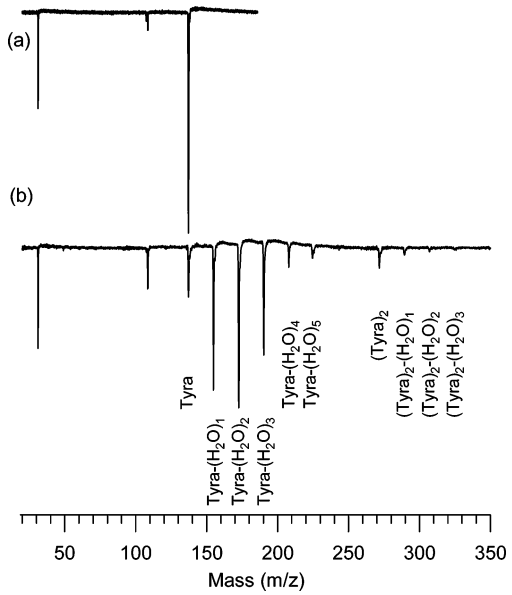

Figure 1. Typical TOF mass spectra obtained by expanding (a) with pure Ar and (b) a mixture of Ar and water vapor. Mass peaks of tyramine, tyramine dimer, and their water clusters are indicated. The two mass peaks occurring before that of tyramine correspond to the fragments from the dissociation of the $C_\beta-C_\alpha$ bond of the ethylamine group in tyramine.

using our frequency-doubled étalon-narrowed pulsed dye laser with a moderate resolution of 0.04 cm^{-1}, because it has very little effect on the moment of inertia and significantly reduces the side chain conformational effect on the transition-moment (TM) rotation.[13] In this case, hydration can be an alternative approach toward more detailed conformational assignment. We have found that the intermolecular hydrogen bonding in the most stable pair of monohydrated clusters is sensitive to the orientation of the phenolic OH group. This leads to more detailed conformational assignments of the monohydrated cluster pair regarding the orientation of the phenolic OH group.

2. Procedures

2.1. Experiment. The experimental setup has been described previously.[15,16] Briefly, tyramine samples were heated to 140 °C and were coexpanded with Ar carrier gas (stagnation pressure, 70 Torr) through a pulsed nozzle (diameter, 0.8 mm) to generate a supersonic jet, which was collimated by a skimmer before entering the ionization chamber. To hydrate tyramine, Ar gas was passed through a water bottle maintained at room temperature. In this controlled situation, we were able to generate hydrated clusters of tyramine$-(H_2O)_{n=1-5}$ and (tyramine)$_2-(H_2O)_{n=1-3}$. Two-color mass-resolved R2PI and UV−UV ion-dip spectra of tyramine and its monohydrated cluster were recorded using two frequency-doubled dye lasers pumped by Nd:YAG lasers. The resulting ions were detected in a linear time-of-flight (TOF) mass spectrometer. Figure 1a shows the typical TOF mass spectrum obtained by expanding with pure Ar. The strong peak at $m/z = 137$ corresponds to tyramine ions. Figure 1b shows the TOF spectrum obtained by expanding with a mixture of Ar and water vapor. Mass peaks of tyramine, tyramine dimer, and their water clusters are indicated therein. The two mass peaks in front of a strong tyramine mass peak are due to the fragmentation of the $C_\beta-C_\alpha$ bond of ethylamine side chain in tyramine. Dissociative ionization or partial thermal decomposition may be responsible for them. For the UV−UV ion-dip spectra, the first burn laser with

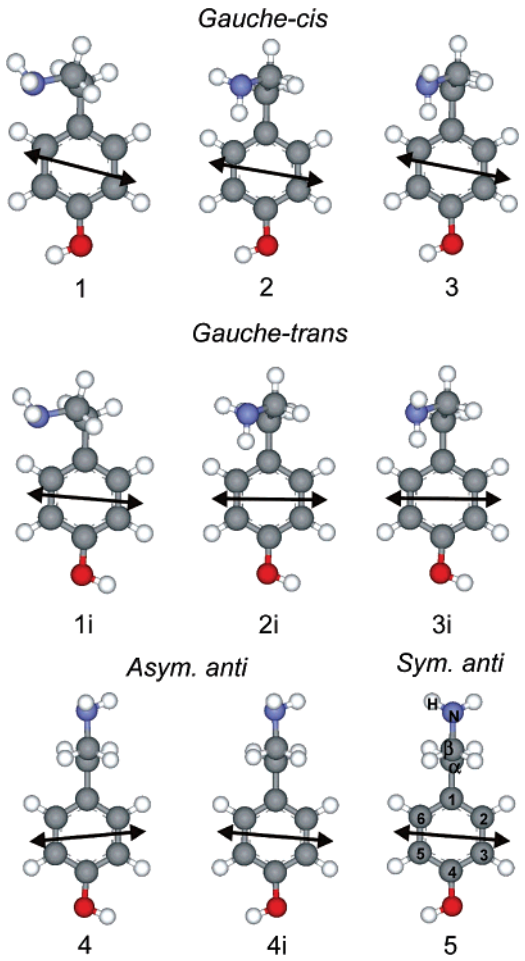

Figure 2. Conformational structures of the nine lowest energy conformers of tyramine predicted by MP2/6-31G** calculations. The arrows show the projection of the TM alignments predicted by CIS/6-31G** calculations on the benzene rings. 1−5 represent conformation of the ethylamine chain, and i indicates the conformers with different orientation of the OH group. In the structure 5, the aromatic carbon atoms are numbered and the atoms defining ethylamino torsional angles (τ_1, τ_2, and τ_3 in Table 1) are labeled "α", "β", "N", and "H".

pulse energy over 1 mJ was scanned and the second weak counterpropagating laser probing the ion-dip signal was delayed by ~70 ns with the frequency fixed to the origin band of each conformer. The frequency-doubled étalon-narrowed excitation laser (Lambda Physik Scanmate 2E, fundamental line width ~0.02 cm^{-1}) was used for high-resolution rotational band contour scans. The pulse energy of the excitation laser was limited to 1 μJ/pulse to minimize saturation effects and that of the ionization laser (wavelength 287.5 nm) was 1−2 mJ/pulse with no ion signal from the ionization laser only. Wavelength calibrations for rotational band contour scans were conducted by simultaneously recording the LIF spectrum of I_2.[17]

2.2. Computation. The ab initio calculations were conducted using Gaussian 03.[18] The geometry optimization and the calculation of relative energies (with zero-point energy correction) of tyramine conformers and their monohydrated clusters in the electronically ground state were performed at the MP2/6-31G** level of theory. For each optimized structure, a local minimum was verified by the absence of any imaginary vibrational frequencies. CIS/6-31G** level calculations were done for the electronically excited states. The ground- and excited-state rotational constants and TM compositions generated from the ab initio calculations were employed to simulate

TABLE 1: Molecular Parameters of Tyramine Predicted from ab Initio Calculations

	1	1i	2	2i	3	3i	4	4i	5
E_{rel}/kJ·mol^{-1} [a]	6.88	7.23	0.63	0.59	0.00	0.34	5.06	4.91	3.61
E_{rel}/kJ·mol^{-1} [b]			0.71	0.00	0.36	0.66	5.94	5.78	4.22
E_{rel}/kJ·mol^{-1} [c]	7.99	8.42	1.00	0.94	0.00	0.38	6.16	6.33	4.92
A''/MHz[a]	3237.7	3232.7	3094.9	3090.9	3132.1	3131.6	4189.4	4189.0	4143.3
B''/MHz[a]	727.5	728.2	737.1	738.2	744.4	745.3	604.6	604.6	603.6
C''/MHz[a]	641.4	641.7	681.8	681.6	681.9	680.1	560.8	560.9	560.2
A''/MHz[c]	3246	3241	3088	3084	3129	3127	4183	4251	4133
B''/MHz[c]	724	725	735	736	742	743	603	595	602
C''/MHz[c]	637	637	681	681	680	678	560	551	559
A'/MHz[d]	3096.7	3102.6	3055.7	3059.1	3093.5	3100.9	4067.7	4069.2	4033.0
B'/MHz[d]	718.5	716.7	727.1	726.9	730.8	730.1	609.5	609.5	609.0
C'/MHz[d]	665.3	668.2	671.6	671.9	668.8	667.9	563.0	562.9	562.6
μ_a^2:μ_b^2:μ_c^2 [d]	7:85:8	1:95:4	4:88:8	0:94:6	6:85:9	1:93:6	1:99:0	1:99:0	1:99:0
θ_{elec}/deg[d,e]	14.5	4.8	9.5	0.4	10.8	1.0	−5.2	4.7	4.5
$\tau_1(C_\beta C_\alpha C_1 C_2)$/deg[a,f]	101.3	101.4	80.9	81.5	84.1	85.5	89.6	86.7	86.9
$\tau_2(NC_\beta C_\alpha C_1)$/deg[a,f]	69.5	69.2	60.3	60.2	61.9	62.1	177.7	177.8	−179.9
$\tau_3(HNC_\beta C_\alpha)$/deg[a,f]	−170.2	−170.3	59.6	59.6	−67.0	−67.1	−176.7	−177.0	57.8
$R_{NH\cdots\pi C}$/Å[a]			2.78	2.77	2.69	2.67			
θ_{elec}/deg[b,e]			−13.5	12.0	−13.5	13.0	1.5	2.0	1.0
τ_1/deg[b,g]			108.9	79.7	103.2	85.0	89.9	91.9	90.1
τ_2/deg[b,g]			66.1	61.6	68.2	62.1	183.3	181.4	180.6
τ_3/deg[b,g]			59.9	56.6	174.6	171.5	171.8	178.2	59.3
$R_{NH\cdots\pi C}$/Å[b]			3.113	2.98	3.827	2.829			

[a] Our work from the MP2/6-31G** calculation. [b] Reference 13. [c] Reference 14. [d] Our work from the CIS/6-31G** calculation. [e] θ_{elec} is defined as the angle between the transition moment and the short axis of the benzene ring. [f] τ_1, τ_2, and τ_3 are torsional angles of an ethylamine chain. The atoms defining these angles (C_1, C_2, C_α, C_β, N, and H) are indicated on structure 5 in Figure 2. [g] τ_1, τ_2, and τ_3 are torsional angles of an ethylamine chain. The atoms defining these angles are indicated in Figure 1 of ref 13.

the rotational band contour spectra of the $S_1 \leftarrow S_0$ origin bands of conformers. We used a PGOPHER program for the simulations.[19]

3. Results and Discussion

3.1. Tyramine. Figure 2 shows the optimized structures of the nine lowest energy conformers of tyramine at the MP2/6-31G** level and the TM alignments calculated at the CIS/6-31G** level. Conformational structure of tyramine is determined by both the structure of the ethylamine chain and the relative orientation of the OH group. Rotation about the $C_\beta-C_\alpha$ bond in the ethylamine chain gives gauche (1−3) or anti (4, 5) conformations. The gauche conformers are divided into three groups according to the 3-fold rotation about the $N-C_\beta$ bond, and each group has cis and trans conformations depending on the relative orientation of the NH_2 and OH groups ((1, 1i), (2, 2i), (3, 3i)). "i" indicates the trans conformation. The anti conformers are divided into two groups, asymmetric (4, 4i) and symmetric (5), according to the rotation about the $N-C_\beta$ bond. The two asymmetric anti conformers differ in the orientation of the OH group. Table 1 summarizes the calculated relative energies, rotational constants in S_0 and S_1 states, $S_1 \leftarrow S_0$ TM components and angles, important geometrical parameters for the nine stable conformers, and those reported by previous works.[13,14]

To estimate the reliability of our calculations, we compare our results with previous works on tyramine[13,14] and related molecules[10,12] in terms of relative energies, geometrical parameters, and direction of TM. Regarding the number of stable conformers and their relative energies, Melandri and Maris predicted nine stable conformers and their relative energies at the MP2/6-31G* level of theory.[14] Their results agree well with ours. The relative energies are dominantly governed by the conformation of the ethylamine side chain. The orientation of the OH group doubling the gauche and asymmetric anti conformers has little effect on the relative energies. The most stable conformer pair is (3, 3i) and the structure 3 is slightly more stable. The structures 1 and 1i with unfavorable interaction between the lone pair electrons of the NH_2 group and the π-electron system on a benzene ring are most unstable. This is also consistent with the theoretical results of *p*-MPEA[12] and PEA.[10] Nine stable conformers of *p*-MPEA and their relative energies predicted at the MP2/6-31G** level of theory are very similar to our results of tyramine.[12] For PEA, the relative energies of five stable conformers predicted by MP2/6-311G** calculations match well with those of conformer pairs of tyramine.[10] Richardson et al. reported seven structures of tyramine by MP2/6-31G** calculations.[13] They considered that the structures corresponding to 1 and 1i were not in minima on the potential energy surface. Regarding the geometrical parameters, we can compare the calculated rotational constants in S_0 and S_1 states with the previous results. Melandri and Maris reported both the calculated and experimental (microwave-determined) rotational constants, A'', B'', and C''.[14] Both the calculated and experimental values agree with our calculated values within 1.8%. For the S_1 rotational constants, A', B', and C', although there are no previously reported values, we can compare the ΔA ($=A' - A''$), ΔB ($=B' - B''$), and ΔC ($=C' - C''$) values with the calculated values of PEA[10] and the experimental values of *p*-MPEA.[12] Upon the $S_1 \leftarrow S_0$ excitation of tyramine, our calculations show that the rotational constants, *A*'s, of conformers decrease by 2% and the *B* and *C* values change by less than 1%. In the case of PEA, the S_0 and S_1 rotational constants were predicted from MP2/6-311G** and CIS/6-31G* calculations, respectively.[10] The *A* values decrease by 3.5% and the *B* and *C* values decrease by 1%. For *p*-MPEA, the experimentally determined ΔA, ΔB, and ΔC are about −4.4, 0.2, and 0.0%, respectively.[12] Our calculated directions of TM are also consistent with those reported for PEA[10] and *p*-tyrosol[20] in the effects of the side chain conformation and the orientation of the phenolic OH group.

Figure 3a and b shows low-resolution R2PI spectra of tyramine in the region of the $S_1 \leftarrow S_0$ origin bands obtained by expanding with Ar carrier gas and a mixture of Ar gas and water

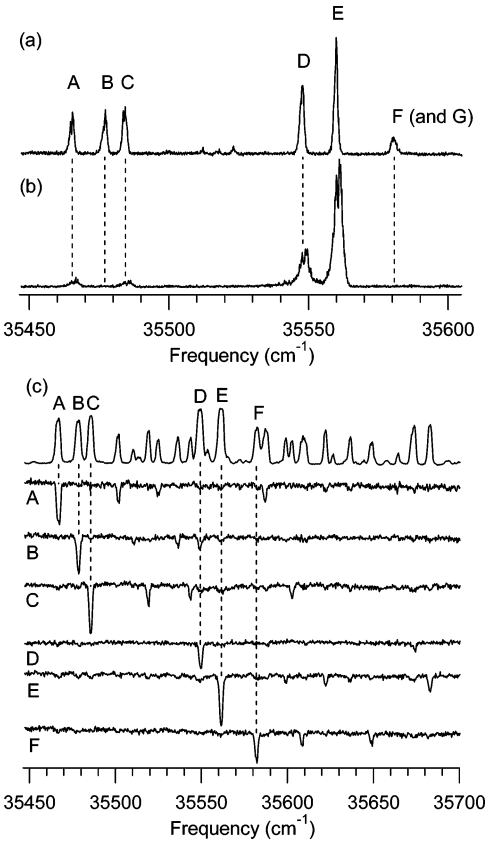

Figure 3. Low-resolution mass-resolved R2PI spectra recorded at the mass of bare tyramine by expanding with (a) Ar carrier gas, (b) a mixture of Ar and water vapor, and (c) UV−UV ion-dip spectra obtained by probing depletion on the bands labeled A−F. For the spectra in a and c, the Ar backing pressure was 70 Torr. The pure Ar gas was passed through a water bottle maintained at room temperature before entering a vacuum chamber for the spectrum in b. For these spectra, tyramine samples were heated to 140 °C.

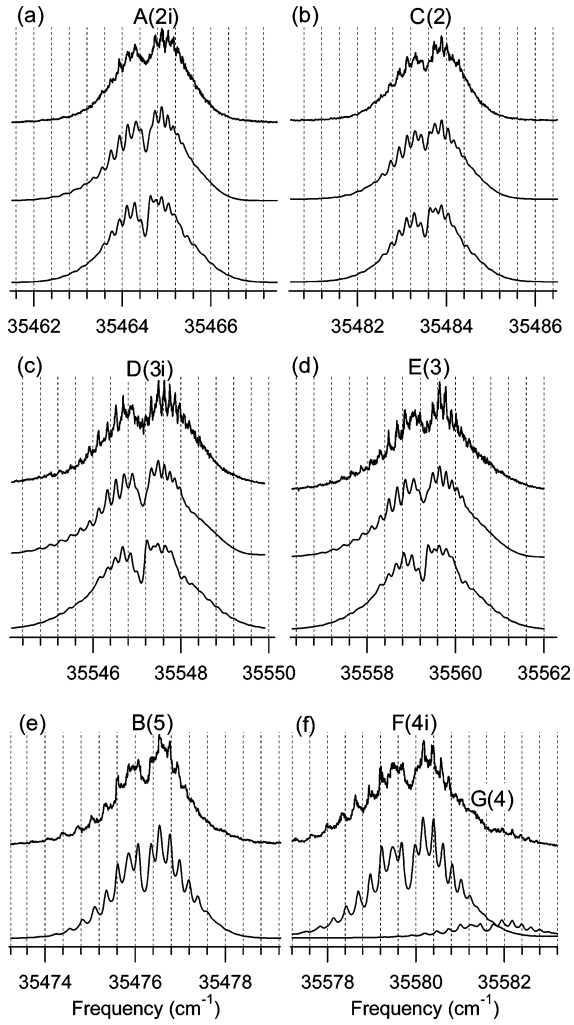

Figure 4. Comparison of experimental rotational band contours of tyramine conformers, A−G. The experimental contours of A, C, D, E, B, F, and G are compared with the simulations assuming their structures to be 2i, 2, 3i, 3, 5, 4i, and 4, respectively. Top traces are the experimental contours. Middle and bottom ones in (a−d) are the simulations from the scaled parameters (see Table 2) and the ab initio data (see Table 1), respectively. The experimental contours are obtained with 70 Torr of the Ar backing pressure. Tyramine samples were heated to 140 °C for A, B, C, F, and G and to 159 °C for D and E. The higher rotational temperatures simulated for D and E are attributed to the higher temperature at which tyramine samples were heated (see Table 2). The rotational structures were convoluted with Voigt line shape profile with 0.05 cm^{-1} Gaussian and 0.08 cm^{-1} Lorentzian components. The former corresponds to a laser line width monitored simultaneously by an external monitor étalon (FSR = 0.25 cm^{-1}). The latter may come from torsion/inversion splittings of terminal groups.

vapor, respectively. Figure 3c shows UV−UV ion-dip spectra obtained by probing depletion on the bands labeled A−F. The UV−UV ion-dip spectra reveal at least six stable conformers in the gas phase. Previous studies have predicted seven stable conformers of tyramine in the gas phase,[7,13] although the $S_1 \leftarrow S_0$ origin bands of the seventh conformers has not been clearly distinguished. The seventh conformer origin band, G, seems to overlap F within 2 cm^{-1} in the low-resolution R2PI spectrum (see Figure 3). Figure 4 compares the experimentally obtained rotational contours of A−G bands with simulated contour spectra. Assuming the conformational assignments of tyramine parallel those of *p*-MPEA,[7,12] the experimental contours of A, C, D, and E bands (top traces in Figure 4a−d, respectively) are compared with two kinds of simulations (middle and bottom traces in Figure 4). For the middle traces, the ground-state rotational constants (A'', B'', and C'') were taken from the microwave data reported by Melandri and Maris,[14] the excited-state rotational constants (A', B', and C') were scaled by the factors $(A' - A'')/A''$, $(B' - B'')/B''$, and $(C' - C'')/C''$ in *p*-MPEA,[12] and the TM components of *p*-MPEA[12] were adopted without modification. The bottom traces are the simulation generated from ab initio data of the corresponding structures. For the anti conformers, B, F, and G, the microwave data have not been reported yet. Their experimental origin band contours (upper traces in Figure 4e and f) are compared with only the simulations with ab initio data (lower traces in Figure 4e and f). The band parameters used for the simulations are listed in Table 1 (ab initio data) and 2 (for the simulations of A, C, D, and E bands: microwave and scaled rotational constants and TM components, for all bands: band origins and T_{rot}). The close-lying F and G origin bands have been resolved in Figure 4f. We can assign the conformation of the ethylamine chain of the A−G conformers as the gauche (A, C, D, and E) and the anti (B, F, and G) conformers by the result of these simulations. Tyramine is a near prolate top rotor molecule ($\kappa = (2B - A - C)/(A - C) = -1$). The theoretically calculated κ values of tyramine conformers are −(0.993−0.976) from A'', B'', and C'' values in Table 1. From the experimental rotational contours, the $^{\Delta Ka}Q_{Ka''}$ subband head spacings ($\approx 2A'' - (B'' + C'')$) are obtained as ∼0.17 cm^{-1} for A, C, D, and E bands and ∼0.23 cm^{-1} for B, F, and G bands. The calculated rotational constants predict the $^{\Delta Ka}Q_{Ka''}$ subband head spacings to be 0.16 cm^{-1} for gauche (2, 2i, 3, and 3i) and 0.24 cm^{-1} for anti conformers (4,

TABLE 2: The Ground- and Excited-State Rotational Constants and TM Components Used for Simulating A, C, D, and E Bands and Band Origin and T_{rot} for Simulating A−G Bands

	A(2i)	B(5)	C(2)	D(3i)	E(3)	F(4)	G(4i)
A″/MHz[a]	3108.179		3110.376	3134.843	3134.884		
B″/MHz[a]	725.58		724.69	733.014	732.20		
C″/MHz[a]	678.02		678.237	678.175	679.40		
A′/MHz[b]	2979.842		3011.964	3015.092	3029.928		
B′/MHz[b]	727.07		723.62	733.285	732.60		
C′/MHz[b]	679.22		678.773	677.639	680.74		
μ_a^2:μ_b^2:μ_c^2 [c]	4:89:7		3:79:18	7:84:9	4:79:17		
origin/cm^{-1} [d]	35464.53	35476.20	35483.53	35547.12	35559.27	35579.82	35581.60
T_{rot}/K[d]	4.0	2.9	3.2	6.5	5.4	4.3	4.3

[a] Reference 14. [b] Values scaled by the factors $(A' - A'')/A''$, $(B' - B'')/B''$, and $(C' - C'')/C''$ of *p*-MPEA (ref 12). [c] Adopted from ref 12. [d] Values that fit contour shapes best.

4i, and 5). Band types of the A−G conformer origin bands do not show significant dependence on the conformation, in contrast to the case of PEA.[10] This is consistent with the calculated TM components, which do not change significantly depending on conformation and have 85−99% of *b* character (see Table 1). Richardson et al. also showed that a phenolic OH group in tyramine effectively reduces the TM rotation.[13] The contours simulated from the scaled band parameters fit the experimental contours of gauche conformers, A, C, D, and E, better than the simulations from ab initio data (see Figure 4a−d). In view of goodness-of-fit, we can compare the residuals of both kinds of fit. The residuals of the simulations from the scaled parameters are smaller than those from the ab initio data (66, 73, 65, and 62% for A, C, D, and E conformers, respectively). One of the main causes of the relatively poor fit of the simulations from our ab initio data is the overestimation of *b* component of TM. The simulations from our ab initio data particularly show large discrepancies from the experimental contours at the central parts of the contours. The simulations from the scaled parameters adopting the TM components of *p*-MPEA without further modification fit better and *b* components of TMs are smaller than those from our ab initio calculations (see Tables 1 and 2). Robertson et al. assigned D and E to the most stable pair of gauche conformers (3 and 3i), A and C to the second most stable pair of gauche conformers (2 and 2i), B to the symmetric anti conformer (5), and F and G to the asymmetric anti conformer pair (4 and 4i).[7] They compared origin band positions and intensities, ionization potentials, and dispersed fluorescence spectra of the conformers of tyramine and the related molecules and revised the earlier assignments of Martinez et al.[5] by swapping bands B and C. Our assignment of the side chain conformation matches well with the assignments of Robertson et al.[7] Also, the observed conformer origin band intensities in our R2PI spectrum (see Figure 3a) and the calculated relative energies (listed in Table 1) dominated by the side chain conformation agree well with these assignments. Comparison of Figure 3a and b provides interesting hints about the conformational effects. When tyramine is expanded with water (see Figure 3b), the relative intensities of the conformer origin bands are drastically changed. We found two kinds of conformational effects on hydration on the basis of the above conformational assignments, the effects of (1) the conformation of the ethylamine chain (gauche or anti) and (2) the relative orientation of the OH group (cis or trans) in the most stable conformer pair, D and E. One of the most striking changes on hydration is that the intensities of the bands B and F, corresponding to anti conformers, decrease below the noise level. This suggests that the anti conformers are more open to hydration and allows us to assign the conformers, A and C, as gauche and the B as anti consistently. Another difference between Figure 3a and b is that the relative intensities of D and E, the most stable pair of gauche conformers (3 and 3i), are changed from 1:1.7 to 1:3.4 on hydration, which means that the hydration has a preference depending on the orientation of the OH group. Because the relative intensities of the second most stable pair of gauche conformers, A and C, do not change as much, this conformational preference seems to require a special orientation of the NH_2 group at the end of the ethylamine chain. Therefore, we might infer the structure of multiply hydrated tyramine by water molecules interconnecting both NH_2 and OH groups. These findings encourage IR−UV ion-dip spectroscopy of multiply hydrated tyramine to reveal the intermolecular hydrogen-bonding structure recognizing the conformation of tyramine.

3.2. Monohydrated Tyramine. The calculated structures of tyramine−$(H_2O)_1$ optimized at the MP2/6-31G** level are shown in Figure 5. Among the large number of possible structures of tyramine−$(H_2O)_1$ arising from proton donating and accepting configurations of the NH_2 and OH groups, we considered two kinds of structures with the proton-accepting NH_2 group (PEA-type hydrogen bonding) and the proton-donating OH group (phenol-type hydrogen bonding), since they were reported as the lowest energy configurations in cases of PEA−$(H_2O)_1$[11] and phenol−$(H_2O)_1$.[21, 22] Figure 5a shows the former PEA-type clusters and b shows the latter phenol-type clusters. Table 3 summarizes the calculated molecular parameters.

Figure 6 shows the low-resolution R2PI spectrum of monohydrated tyramine and UV−UV ion-dip spectra obtained by probing depletion on the bands labeled H−N. The UV−UV ion-dip spectra reveal the seven kinds of stable monohydrated clusters, H−N, in the gas phase. The observed $S_1 \leftarrow S_0$ origin bands can be divided into two groups according to their spectral shifts from those of tyramine. The first group, including H−L, shows significant red shifts and the second group, including M and N, shows slight blue shifts. In Table 4, the origin band positions of tyramine and tyramine−$(H_2O)_1$ and the spectral shifts observed in our R2PI spectra are listed. According to previous studies on the spectral shifts of phenol−$(H_2O)_1$[21] and *p*-cresol−$(H_2O)_1$,[23] the excited state is more stabilized when the OH group acts as a proton donor (an increase of electron density at the O atom), since the $\pi-\pi^*$ transition transfers electron density from the O atom to the chromophore ring. This results in a red-shifted $S_1 \leftarrow S_0$ origin band of the cluster from that of the monomer. The magnitude of spectral shifts of the red-shifted group in our R2PI spectrum of tyramine−$(H_2O)_1$ (see Table 4) and that of phenol−$(H_2O)_1$ reported by Berden et al. (-353 cm^{-1})[21] are very similar. Assuming the constant shift ($\sim$350 cm^{-1}) induced by the phenol-type intermolecular hydrogen bonding, we can correlate the conformation of tyramine in tyramine−$(H_2O)_1$ parallel with that of bare tyramine (H−A, I−B, J−C, K−D, and L−E) tentatively. The blue-shifted origin

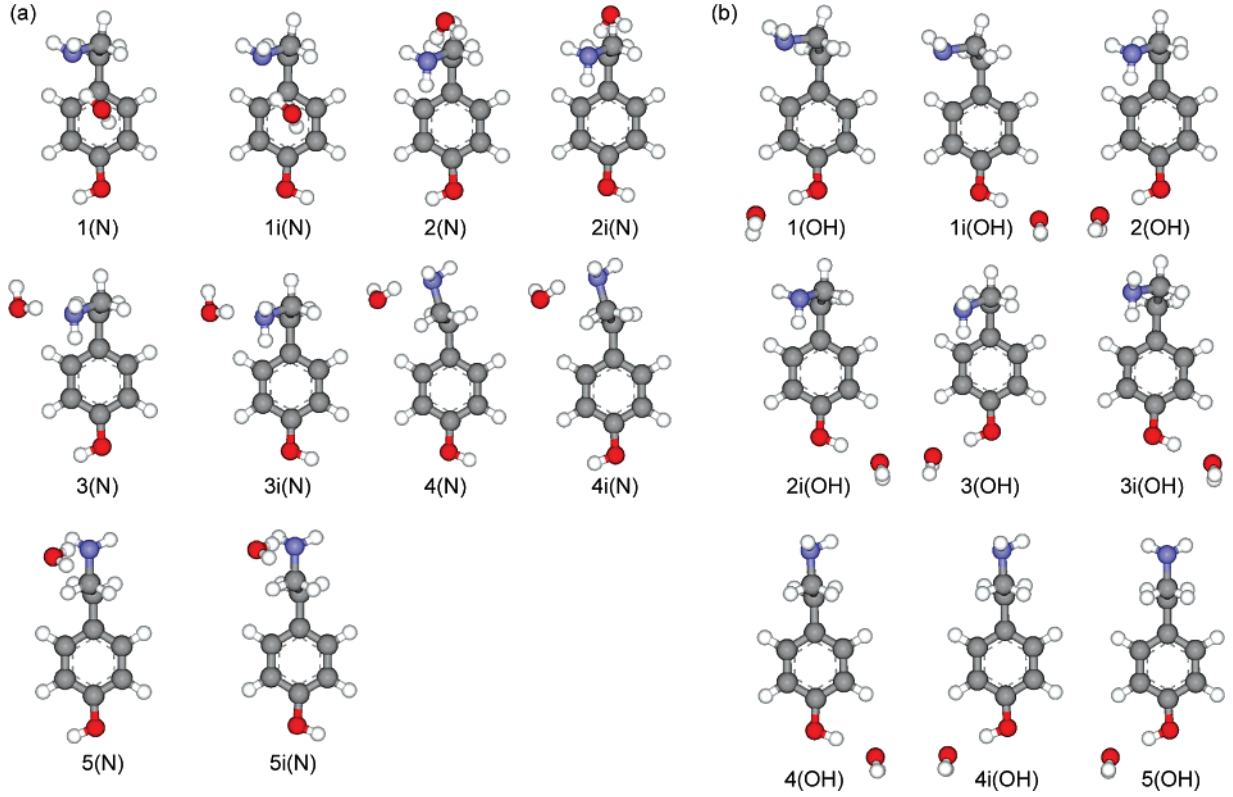

Figure 5. Conformational structures of tyramine−$(H_2O)_1$ predicted by the MP2/6-31G** calculation. (a) The structures in which a N atom on the ethylamine chain is used as the binding site for a proton-donating water molecule, and (b) those in which the OH group is used as the binding site for a proton-accepting water molecule.

TABLE 3: Molecular Parameters of Monohydrated Tyramine Predicted from the MP2/6-31G Calculations**

conformer	1(N)	1i(N)	2(N)	2i(N)	3(N)	3i(N)	4(N)	4i(N)	5(N)	5i(N)
E_{rel}/kJ·mol^{-1}	9.42	9.72	10.99	10.91	0.00	1.30	10.81	10.18	15.34	15.65
E_{bind}/kJ·mol^{-1} [a]	36.36	36.41	28.54	28.57	38.90	37.94	33.15	33.63	27.18	26.87
E_{bind}/ kJ·mol^{-1} [a,b]	15.25	15.17	15.91	16.05	18.13	17.23	13.54	13.98	13.90	13.62
A''/MHz	1843.4	1848.7	2204.4	2179.6	1785.7	1791.1	2241.2	2241.6	2132.3	2136.7
B''/MHz	664.6	662.9	421.8	423.8	598.9	597.0	488.2	488.6	401.8	401.7
C''/MHz	618.4	618.7	415.6	416.8	502.3	501.6	421.8	422.0	374.4	373.2
$R_{N\cdots HOH}$/Å	2.01	2.00	1.94	1.94	1.94	1.94	1.96	1.96	1.96	1.96
$R_{NH\cdots\pi C}$/Å			2.80	2.78	2.72	2.71				
$R_{C(ring)H\cdots OH}$/Å					2.42	2.43	2.91	2.90		

conformer	1(OH)	1i(OH)	2(OH)	2i(OH)	3(OH)	3i(OH)	4(OH)	4i(OH)	5(OH)
E_{rel}/kJ·mol^{-1}	15.72	15.98	7.13	7.09	7.22	7.55	12.49	12.33	10.67
E_{bind}/kJ·mol^{-1} [a]	30.07	30.15	32.40	32.40	31.67	31.69	31.47	31.48	31.84
E_{bind}/ kJ·mol^{-1} [a,b]	18.95	19.03	21.31	21.33	20.63	20.59	20.37	20.41	20.75
A''/MHz	2005.2	2561.2	2101.9	2268.2	2123.7	2352.9	2669.4	2649.6	2610.1
B''/MHz	483.5	440.6	479.8	461.1	481.7	459.0	402.1	403.1	403.4
C''/MHz	411.2	402.6	426.8	427.6	426.7	424.1	365.2	365.7	365.9
$R_{NH\cdots\pi C}$/Å			2.77	2.77	2.67	2.66			
$R_{C(ring)OH\cdots OH}$/Å	1.87	1.87	1.86	1.86	1.86	1.86	1.86	1.86	1.86
$R_{C(ring)H\cdots OH}$/Å	2.73	2.74	2.71	2.70	2.70	2.71	2.72	2.71	2.71

[a] Binding energies were calculated from the relative energy difference of a cluster and fragments with zero-point energy correction. $E_{bind} = E(AB) - E(A) - E(B)$, where $E(AB)$ is the relative energy of a cluster and $E(A)$ and $E(B)$ are those of fragments at their optimized structures, respectively. [b] Basis set superposition error (BSSE) correction was taken from the MP2/6-31G** calculation.

bands, M and N, whose intensities are stronger than those of the red-shifted bands, show a relatively small magnitude of spectral shifts. This might be attributed to the PEA-type hydrogen bonding as suggested by Teh and Sulkes.[4] Since the NH_2 group at the end of the ethylamine chain is farther from the chromophore ring than the OH group, the effect of perturbation on the electronic structure of the chromophore by the NH_2 group would be weaker than by the OH group. Hockrigde and Robertson observed that the origin band of the most stable PEA−$(H_2O)_1$ conformer with the NH_2 group as a proton acceptor is blue-shifted by 23 cm^{-1} from that of the related (most stable) PEA conformer[11] and also Fernández et al. reported two conformer origin bands of *p*-MPEA−$(H_2O)_1$ which are blue-shifted by ∼70 cm^{-1} from those of the most stable pair of *p*-MPEA conformers.[24] Another noticeable observation is the origin band intensity distributions in both groups. The red-shifted group shows a similar origin band intensity distribution to that of tyramine, while the blue-shifted group shows only two strong origin bands. Therefore, we expect that the phenol-type hydrogen bonding does not change the

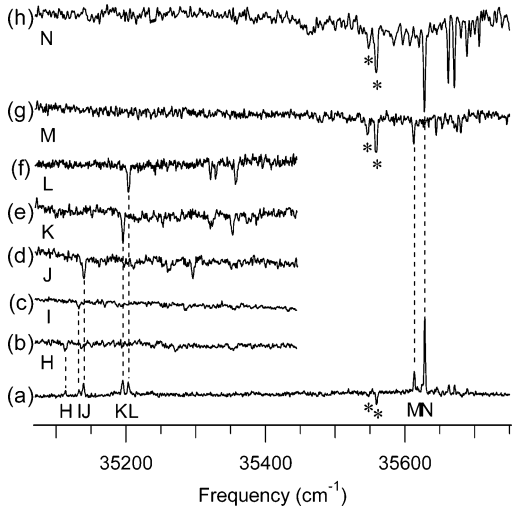

Figure 6. (a) Low-resolution mass-resolved R2PI spectra recorded at the mass of tyramine$-(H_2O)_1$ and (b−h) UV−UV ion-dip spectra obtained by probing depletion on the bands labeled H−N in a. Ion dips denoted by "*" at band positions of bare tyramine conformers D and E in a, g, and h are due to MCP detector saturation.

TABLE 4: Origin Band Positions of Bare Tyramine and Tyramine$-(H_2O)_1$ and the Spectral Shifts of the Origin Bands of Tyramine$-(H_2O)_1$ from That of the Related Bare Tyramine Conformer

bare tyramine		tyramine$-(H_2O)_1$		
conformer	origin position (cm^{-1})	conformer	origin position (cm^{-1})	spectral shifts (cm^{-1})
A	35 465	H	35 113	−352 from A
B	35 476	I	35 133	−343 from B
C	35 484	J	35 139	−345 from C
D	35 547	K	35 195	−352 from D
E	35 559	L	35 203	−356 from E
F	35 580	M	35 613	+66 from D
G	35 582	N	35 629	+70 from E

conformational hypersurface significantly, but the PEA-type hydrogen makes that hypersurface steeper. These observations and interpretations are consistent with the results of ab initio calculations. Figure 7 shows the relative energies E_{rel} and the binding energies E_{bind} of the monohydrated clusters. The E_{rel} of the phenol-type clusters in the right side of Figure 7 shows a similar trend to that of E_{rel} of tyramine, but that of the PEA-type clusters in the left side of Figure 7 shows a considerably different trend (compare the relative energies of both cluster groups with those of bare tyramine conformers in Table 1). The PEA-type clusters, 3(N) and 3i(N), are particularly stabilized, so the structures of the two strong blue-shifted M and N can be assigned to them. The conformations of tyramine in these most stable monohydrated clusters are those of D and E, the most stable gauche conformer pair. We can obtain more detailed conformational assignments regarding the orientation of the phenolic OH group by comparing the origin band intensities of the bare tyramine conformers and their monohydrated clusters as follows.

The conformational effect on hydration can provide an alternative approach toward more detailed conformational assignment. The relative intensities of the blue-shifted origin bands, M and N, are in the ratio of 1:3.7. This is considerably larger than that of the related bare tyramine conformers, D and E (1:1.7) (see Figure 3a). From this observation, we deduce that the intermolecular hydrogen bonding in the monohydrated clusters, M and N, is sensitive to the orientation of the phenolic

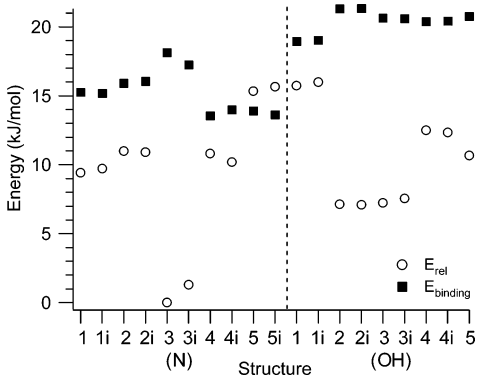

Figure 7. Open circles and filled squares represent relative energies E_{rel} (open circles) and binding energies E_{bind} (BSSE corrected) of tyramine$-(H_2O)_1$, respectively. These values are taken from Table 3. The left side shows E_{rel} and E_{bind} for the PEA-type monohydrated clusters and the right side shows those of the phenol-type ones.

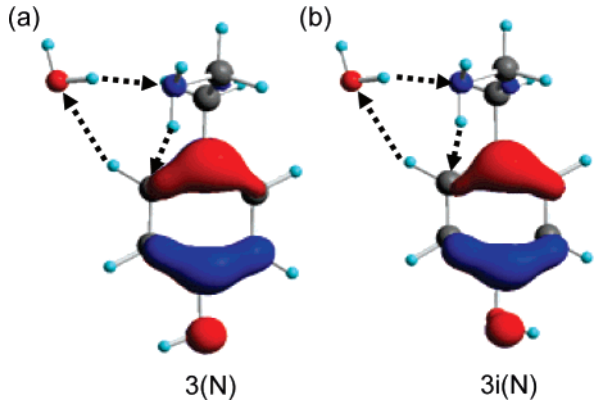

Figure 8. HOMO of the structures, (a) 3(N) and (b) 3i(N), of monohydrated tyramine. Arrows represent the proton-donating direction in the cyclic hydrogen bonding.

OH group, which does not, however, participate in the hydrogen bonding. This is well explained by the combination of the effect of the orientation of the phenolic OH group on the electron density in the highest occupied molecular orbital (HOMO) of tyramine[13] and the cyclic hydrogen-bonding linkage in the structures, 3(N) and 3i(N), predicted by our ab initio calculation. Figure 8 shows the HOMO of 3(N) and 3i(N) with their cyclic hydrogen-bonding structures. The π-electron density at the carbon atom participating in the cyclic hydrogen-bonding linkage depends on the orientation of the phenolic OH group. The 3(N) structure may be further stabilized because the more polarized C−H bond takes part in the cyclic hydrogen-bonding linkage. Thus, we obtain more detailed conformational assignments of M to 3i(N) and N to 3(N).

We obtained the rotational band contours of two strongly observed conformer origin bands, M and N. Figure 9 shows their experimentally obtained rotational band contours along with the calculated structures of 3i(N) and 3(N) of which TM alignments and *b*-axes are projected on the benzene rings. In contrast to the case of tyramine, sharp central peaks indicating a slight *a* character of TM components are observed in band contours of M and N. For the structures 3(N) and 3i(N), the angles, θ_{elec}, between the TM alignment and the short axis of the benzene ring and the TM compositions, $\mu_a^2:\mu_b^2:\mu_c^2$, were obtained from the CIS/6-31G** calculation. The θ_{elec} angles are 16° and 5° and the TM compositions are 29:65:6 and 16:84:0, respectively. The θ_{elec} angles are similar to those of bare tyramine conformers, 3 (11°) and 3i (1°), but the TM compositions change significantly from those of 3 (6:85:9) and 3i

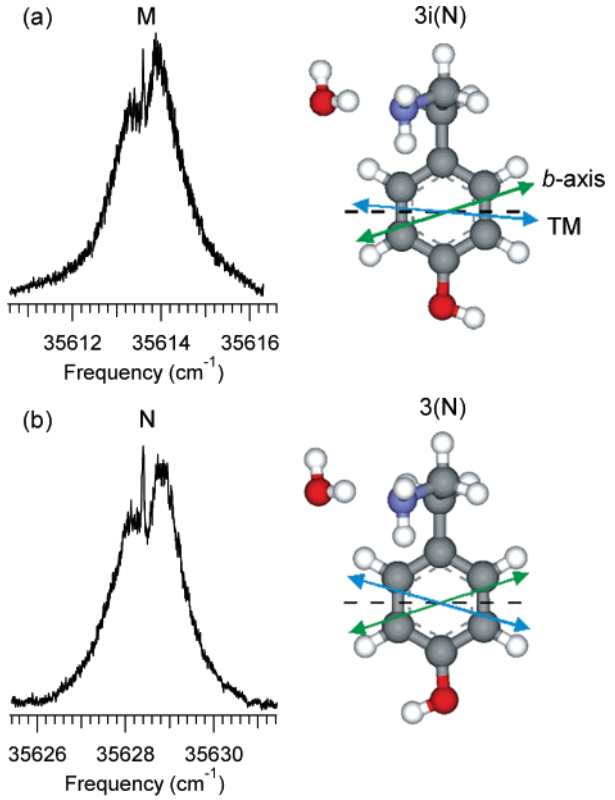

Figure 9. Experimental rotational band contours of monohydrated tyramine conformers, (a) M and (b) N, along with the corresponding calculated structures, 3i(N) and 3(N). On the benzene rings, blue and green arrows represent the TM alignment and *b*-axes, respectively, and the dashed line is the short axis of the benzene ring.

(1:93:6). It is mainly attributed to inertial axis reorientation because of attachment of a water molecule at the N atom of the gauche ethylamine chain.

4. Conclusions

We have assigned gauche or anti conformation of the ethylamine side chain for all seven stable tyramine conformers by UV rotational band contour spectra and ab initio calculations. On the basis of the conformational assignments, two kinds of conformational effects on hydration have been revealed. Seven stable conformers of monohydrated tyramine have been detected. Five conformers showing red shifts of their $S_1 \leftarrow S_0$ origin bands have been suggested to be the phenol-type monohydrated clusters, and two conformers showing blue shifts of their $S_1 \leftarrow S_0$ origin bands have been suggested to be the PEA-type clusters. We also found the effect of the orientation of the phenolic OH group on the cyclic hydrogen-bonding linkage in the most stable pair of monohydrated clusters from the origin band intensities in our R2PI spectrum. This leads to the more detailed conformational assignments on the orientation of the phenolic OH group.

Acknowledgment. We thank KRF for the financial support through ABRL (R14-2005-033-0100) and KOSEF through the Center for Intelligent Nano-Bio Materials (R11-2005-008-00000-0). S.L. thanks the Korea Research Foundation (KRF-2006-311-C00078) for financial support.

References and Notes

(1) Alberts, B.; Bray, D.; Lewis, J.; Raff, M.; Roberts, K.; Watson, J. D. *Molecular Biology of the Cell*, 3rd ed.; Garland Publishing: New York, 1994.
(2) Robertson, E. G.; Simons, J. P. *Phys. Chem. Chem. Phys.* **2001**, *3*, 1 and references therein.
(3) Zwier, T. S. *J. Phys. Chem. A* **2006**, *110*, 4133.
(4) Teh, C. K.; Sulkes, M. *J. Chem. Phys.* **1991**, *94*, 5826.
(5) Martinez, S. J.; Alfano, J. C.; Levy, D. H. *J. Mol. Spectrosc.* **1993**, *158*, 82.
(6) Unamuno, I.; Fernández, J. A.; Longarte, A.; Castaño, F. *J. Phys. Chem. A* **2000**, *104*, 4364.
(7) Robertson, E. G.; Simons, J. P.; Mons, M. *J. Phys. Chem. A* **2001**, *105*, 9990.
(8) Fernández, J. A.; Unamuno, I.; Castaño, F. *J. Phys. Chem. A* **2001**, *105*, 9993.
(9) Sun, S.; Bernstein, E. R. *J. Am. Chem. Soc.* **1996**, *118*, 5086.
(10) Dickinson, J. A.; Hockridge, M. R.; Kroemer, R. T.; Robertson, E. G.; Simons, J. P.; McCombie, J.; Walker, M. *J. Am. Chem. Soc.* **1998**, *120*, 2622.
(11) Hockridge, M. R.; Robertson, E. G. *J. Phys. Chem. A* **1999**, *103*, 3618.
(12) Yi, J. T.; Robertson, E. G.; Pratt, D. W. *Phys. Chem. Chem. Phys.* **2002**, *4*, 5244.
(13) Richardson, P. R.; Bates, S. P.; Jones, A. C. *J. Phys. Chem. A* **2004**, *108*, 1233.
(14) Melandri, S.; Maris, A. *Phys. Chem. Chem. Phys.* **2004**, *6*, 2863.
(15) Lee, Y.; Yoon, Y.; Baek, S. J.; Joo, D.-L.; Ryu, J.-S.; Kim, B. *J. Chem. Phys.* **2000**, *113*, 2116.
(16) Lee, Y.; Jung, J.; Kim, B.; Butz, P.; Snoek, L. C.; Kroemer, R. T.; Simons, J. P. *J. Phys. Chem. A* **2004**, *108*, 69.
(17) Gerstenkorn, S.; Luc, P. *Atlas du Spectre d'Absorption de la Molécule d'Iode Entre 14800-20000 cm*$^{-1}$; CNRS: Paris, 1978.
(18) Frisch, M. J.; Trucks, G. W.; Schlegel, H. B.; Scuseria, G. E.; Robb, M. A.; Cheeseman, J. R.; Montgomery, J. A., Jr.; Vreven, T.; Kudin, K. N.; Burant, J. C.; Millam, J. M.; Iyengar, S. S.; Tomasi, J.; Barone, V.; Mennucci, B.; Cossi, M.; Scalmani, G.; Rega, N.; Petersson, G. A.; Nakatsuji, H.; Hada, M.; Ehara, M.; Toyota, K.; Fukuda, R.; Hasegawa, J.; Ishida, M.; Nakajima, T.; Honda, Y.; Kitao, O.; Nakai, H.; Klene, M.; Li, X.; Knox, J. E.; Hratchian, H. P.; Cross, J. B.; Bakken, V.; Adamo, C.; Jaramillo, J.; Gomperts, R.; Stratmann, R. E.; Yazyev, O.; Austin, A. J.; Cammi, R.; Pomelli, C.; Ochterski, J. W.; Ayala, P. Y.; Morokuma, K.; Voth, G. A.; Salvador, P.; Dannenberg, J. J.; Zakrzewski, V. G.; Dapprich, S.; Daniels, A. D.; Strain, M. C.; Farkas, O.; Malick, D. K.; Rabuck, A. D.; Raghavachari, K.; Foresman, J. B.; Ortiz, J. V.; Cui, Q.; Baboul, A. G.; Clifford, S.; Cioslowski, J.; Stefanov, B. B.; Liu, G.; Liashenko, A.; Piskorz, P.; Komaromi, I.; Martin, R. L.; Fox, D. J.; Keith, T.; Al-Laham, M. A.; Peng, C. Y.; Nanayakkara, A.; Challacombe, M.; Gill, P. M. W.; Johnson, B.; Chen, W.; Wong, M. W.; Gonzalez, C.; Pople, J. A. *Gaussian 03*, Revision C.02; Gaussian, Inc.: Wallingford CT, 2004.
(19) Western, C. M. PGOPHER, a Program for Simulating Rotational Structure, University of Bristol, http://pgopher.chm.bris.ac.uk.
(20) Hockridge, M. R.; Knight, S. M.; Robertson, E. G.; Simons, J. P.; McCombie, J.; Walker, M. *Phys. Chem. Chem. Phys.* **1999**, *1*, 407.
(21) Berden, G.; Meerts, W. L.; Schmitt, M.; Kleinermanns, K. *J. Chem. Phys.* **1996**, *104*, 972.
(22) Fang, W.-H. *J. Chem. Phys.* **2000**, *112*, 1204.
(23) Pohl, M.; Schmitt, M.; Kleinermanns, K. *J. Chem. Phys.* **1991**, *94*, 1717.
(24) Fernández, J. A.; Unamuno, I.; Longarte, A.; Castaño, F. *J. Phys. Chem. A* **2001**, *105*, 961.